Proceedings of the Symposium A of the European Materials Research, Warsaw, September 2008

Synthesis and Characterization of Mn-Doped $BiFeO_3$ Nanoparticles

H. Fukumura, S. Matsui, N. Tonari, T. Nakamura, N. Hasuike, K. Nishio, T. Isshiki, H. Harima

Department of Electronics, Kyoto Institute of Technology, Kyoto 606-8585, Japan

and K. Kisoda

Department of Physics, Wakayama University, Wakayama 640-8510, Japan

$BiFeO_3$ is a multiferroic material showing antiferromagnetic ordering and ferroelectric behavior simultaneously. Here, Mn-doped $BiFeO_3$ nanoparticles were synthesized up to 10% of Mn composition by a sol-gel process. The samples showed high crystallinity with no secondary phase up to 2% of Mn doping. A phonon peak at 1250 cm^{-1} in undoped $BiFeO_3$ showed anomalous intensity enhancement in the magnetically ordered phase below $T_N = 643$ K due to a spin-phonon coupling. This behavior was less pronounced in the Mn-doped samples, suggesting a suppression of magnetic ordering between Fe^{3+} spins by Mn doping.

PACS numbers: 78.30.Hv, 63.20.D−, 78.30.−j

1. Introduction

There has been increasing interest in so-called multiferroics, showing ferroelectric properties together with ferromagnetic or ferroelastic properties. If ferroelectricity and ferromagnetism coexist, we may expect a crossing effect (so-called magnetoelectric effect) in which the magnetization is controlled by applied electric field or the electric polarization controlled by magnetic field. $BiFeO_3$ now gathers much attention for future device applications because it shows ferroelectricity and weak ferromagnetism (antiferromagnetism in reality with canted spin pairs) above room temperature (Curie temperature $T_C = 1103$ K and Néel temperature $T_N = 643$ K) [1–3].

Many research groups have tested substitution of other elements for the Bi- and/or Fe-site to enhance the ferroelectric and magnetic orderings [4–7]. As a typical result, $BiFeO_3$ thin films have greatly increased their remnant electric polarization by doping with Mn [8]. However, the mechanism has not yet been clarified and, furthermore, the doping effect on the magnetic ordering is left an open question. A good approach to elucidate this problem is to prepare Mn-doped samples at different doping levels with a substrate-free condition. From this viewpoint, we have synthesized Mn-doped $BiFeO_3$ powder samples by a sol-gel process with Mn content of 0–10%, and investigated their lattice properties by X-ray diffraction (XRD), transmission electron microscopy (TEM), and Raman scattering.

2. Experiment

Mn-doped $BiFeO_3$ particles with [Mn] = 0–10% were prepared using a sol-gel method based on a glycol-gel reaction [9]: $Bi(NO)_3 \cdot 5H_2O$, $Fe(NO)_3 \cdot 9H_2O$ and MnF_3 were mixed in ethylene glycol. The mixture was stirred at 80°C and the resultant gel samples were preheated to 400°C at a ramp rate of 5°C/min to remove the excess CH_x and NO_x impurities. Finally, the samples were annealed at 600°C in air for 30 min.

Crystal structure and morphology of the samples were observed by XRD and TEM, and selected area electron diffraction (SAED), and the sample composition was studied by energy dispersive X-ray (EDX) analysis. For phonon properties, microscopic Raman scattering measurement was performed at 300–800 K using an Ar^+ laser at 514.5 nm for excitation. The scattered light was analyzed by a double monochromator of focal length 85 cm with a liquid-N_2-cooled CCD (charge coupled device) detector.

3. Results and discussion

Figure 1a shows XRD patterns for the Mn: $BiFeO_3$ samples with content of [Mn] = 0, 1, 2, 3, 5, and 10%. The result indicates that the $BiFeO_3$ samples had a perovskite-based rhombohedral structure as reported before [10] and no secondary phases were included up to 2%. At Mn contents larger than 3%, small impurity components appeared (see asterisks in Fig. 1a). Figure 1b shows a magnified pattern around $2\theta = 32°$. As shown in this figure, (104) and (110) peaks are clearly separated in the undoped $BiFeO_3$ sample. With increasing the Mn content from 0 to 3%, the (104) peak shifts to higher angle, while the (110) peak is almost unshifted, then at the Mn content > 5% they merge to a single (110) peak. This result suggests small lattice distortion from the rhombohedral structure of $BiFeO_3$ occurring with increasing Mn content. The same behavior has been reported in

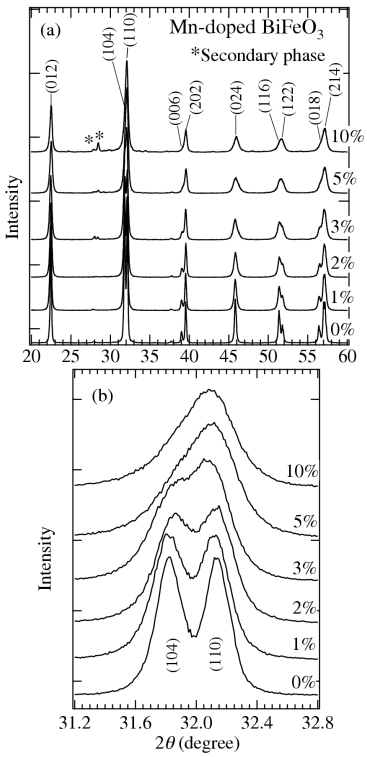

Fig. 1. (a) XRD patterns of Mn-doped $BiFeO_3$ nanoparticles ([Mn] = 0–10%) and (b) magnified patterns in the vicinity of $2\theta = 32°$. Asterisks in (a) denote impurity phase.

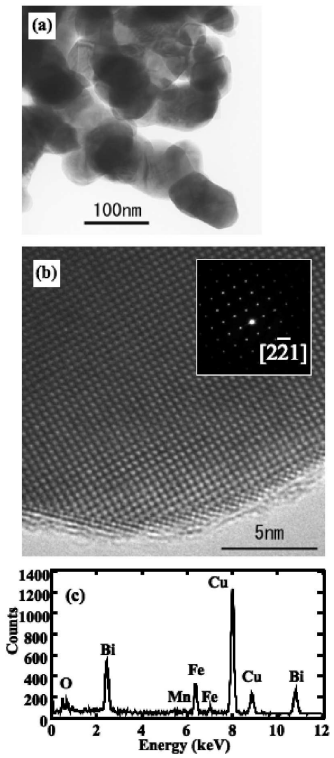

Fig. 2. (a) TEM image of the sample with [Mn] = 2%, (b) its magnified image with SAED pattern, and (c) EDX spectrum.

Mn-doped $BiFeO_3$ film [8], which corresponds to a lattice distortion or phase change from rhombohedral to a monoclinic or a tetragonal structure.

Figures 2a and b show typical TEM images of the sample with Mn content of 2% at different magnifications. The inset of Fig. 2b shows a SAED pattern. Figure 2a shows that the particle size was around 100 nm. As confirmed by the clear lattice image of Fig. 2b, the sample consisted of single crystal particles with high crystallinity. The Mn content was analyzed by EDX analysis as shown in Fig. 2c. The Cu signal is an artifact coming from the sample holder. The Mn content was estimated to $\approx 2\%$ from the intensity ratio of Fe and Mn signals, agreeing with the growth recipe. Recalling that there were no secondary phases for Mn = 2% as seen in XRD patterns in Fig. 1a, our results indicate that the Mn atoms are smoothly incorporated in $BiFeO_3$ host lattice. Similar results were also confirmed for the other samples.

Figure 3a shows Raman spectra of the samples. In the undoped sample (bottom), seven phonon peaks were easily identified and classified to A_1- and E-type modes with reference to a previous result for single crystals as marked in the figure [11]. With increasing Mn content from [Mn] = 0 to 10%, all peaks broadened systematically. The peak broadening derived from a relaxation of lattice periodicity was induced by the incorporation of Mn into the $BiFeO_3$ host lattice. Careful analysis reveals that some phonon modes show anomalous behavior with increasing Mn content: for example, as shown in the expanded spectra in Fig. 3b, the A_1 mode at 135 cm^{-1} due to a stretching vibration of Bi–O bonds [12] shows an abruptly large frequency shift around [Mn] = 3%. It suggests a sudden contraction of the Bi–O bond length, or a small lattice distortion from the rhombohedral structure for undoped $BiFeO_3$. This is consistent with the result of the XRD analysis shown in Fig. 1b.

Figure 4a shows a temperature variation of the Raman spectra for a sample with [Mn] = 2% in the two-phonon peak spectral region between 300 and 800 K. With lowering the temperature from 800 K, the broad peak at $\approx$ 1250 cm^{-1} enhances its intensity. The relative intensity variation is plotted in Fig. 4b by filled triangle. Here, the intensity of the 2-phonon peak has been normalized to the E mode intensity at 470 cm^{-1}. While the intensity change is negligibly small at higher temperatures, it changes prominently at temperatures below $\approx$ 600 K. This temperature is close to the Néel temperature of bulk $BiFeO_3$, T_N = 643 K. This phenomenon has been previously reported in bulk samples and interpreted by a coupling between the phonon and spin systems [11, 13]. According to Ramirez et al. [13], this 2-phonon mode is sensitive to the magnetic phase transition of $BiFeO_3$. Figure 4b shows a comparison of the

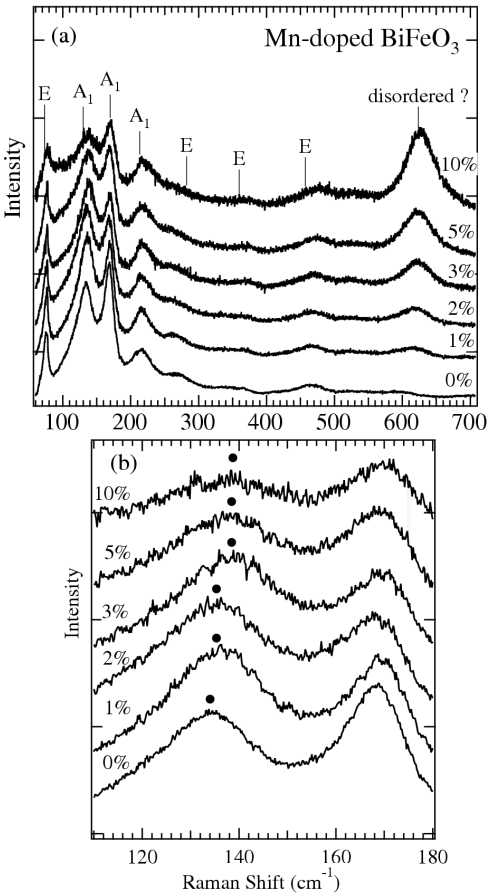

Fig. 3. (a) Raman spectra of Mn-doped $BiFeO_3$ samples ([Mn] = 0–10%) and (b) magnified spectra of A_1 modes at 135 cm^{-1}. The dots in (b) show peak positions determined by curve fitting analysis.

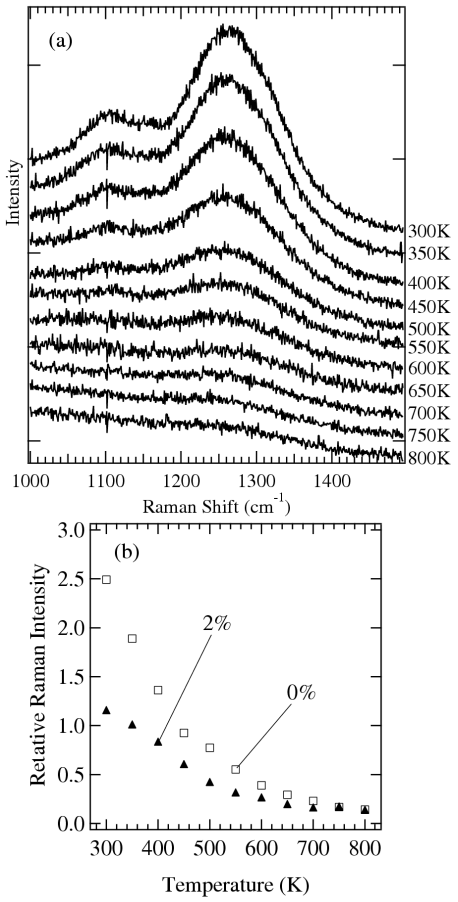

Fig. 4. (a) Temperature variation dependence of the Raman spectra in high frequency (2-phonon) region for [Mn] = 2% between 300 and 800 K, and (b) comparison of the signal intensity variation with temperature between [Mn] = 0 and 2% for the 2-phonon band at 1250 cm^{-1}.

peak intensity variation between [Mn] = 2% (filled triangle) and 0% (open square). The comparison clearly shows that the signal enhancement at low temperatures is lowered by Mn-doping. It means that the coupling between Fe^{3+} spins is suppressed by doping with Mn in $BiFeO_3$. Lattice distortion by doping as suggested in this study (Figs. 1 and 3) may be a possible cause, or Mn ions substituted to Fe sites may directly weaken the antiferromagnetic ordering.

4. Conclusion

Mn-doped $BiFeO_3$ nanoparticle samples were synthesized using a sol-gel process and characterized by X-ray diffraction, transmission electron microscopy, and Raman scattering. The obtained samples were highly crystallized and contained no secondary phases up to 2% of Mn content. With increasing Mn content, the samples showed anomalous behavior at around $\approx 3\%$, suggesting a lattice distortion from the rhombohedral structure to a monoclinic or a tetragonal structure occurred. Raman scattering observation of the samples at 300–800 K showed anomalous intensity enhancement of a 2-phonon signal at temperatures below ≈ 600 K. This was interpreted by spin-phonon coupling in the magnetically ordered phase below $T_N = 643$ K. This behavior was less pronounced in the Mn-doped samples, suggesting a suppression of magnetic ordering of Fe^{3+} spins by doping.

References

[1] G. Smolenskii, V. Yudin, E. Sher, Y.E. Stolypin, *Sov. Phys.-JETP* **16**, 622 (1963).

[2] Y.N. Venevtsev, G. Zhadanov, S. Solov'ev, *Sov. Phys.-Crystallogr.* **4**, 538 (1960).

[3] G. Smolenskii, V. Isupov, A. Agranovskaya, N. Kranik, *Sov. Phys.-Solid State* **2**, 2651 (1961).

[4] X. Qi, J. Dho, R. Tomov, M.G. Blamire, J.L. MacManus-Driscoll, *Appl. Phys. Lett.* **86**, 062903 (2005).

[5] V.R. Palkar, K.G. Kumara, S.K. Malik, *Appl. Phys. Lett.* **84**, 2856 (2004).

[6] D. Lee, M.G. Kim, S. Ryu, H.M. Jang, *Appl. Phys. Lett.* **86**, 222903 (2005).

[7] Y. Wang, C.W. Nan, *Appl. Phys. Lett.* **89**, 052903 (2006).

[8] S.K. Singh, H. Ishiwara, K. Maruyama, *Appl. Phys. Lett.* **88**, 262908 (2006).

[9] T.J. Park, G.C. Papaefthymiou, A.J. Viescas, A.R. Moodenbaugh, S.S. Wong, *Nano Lett.* **7**, 766 (2007).

[10] I. Sosnowska, R. Przenioslo, P. Fischer, V.A. Murashov, *Acta Phys. Pol. A* **86**, 619 (1994).

[11] H. Fukumura, S. Matsui, H. Harima, T. Takahashi, T. Itoh, K. Kisoda, M. Tamada, Y. Noguchi, M. Miyayama, *J. Phys., Condens. Matter* **19**, 365224 (2007).

[12] M.K. Singh, S. Ryu, H.M. Jang, *Phys. Rev. B* **72**, 132101 (2005).

[13] M.O. Ramirez, M. Krishnamurthi, S. Denev, A. Kumar, S.Y. Yang, Y.H. Chu, E. Saiz, J. Seidel, A.P. Pyatakov, A. Bush, D. Viehland, J. Orenstein, R. Ramesh, V. Gopalan, *Appl. Phys. Lett.* **92**, 022511 (2008).